

AD-A170 618

PICOSECOND OPTOELECTRONIC MEASUREMENT OF THE HIGH
FREQUENCY SCATTERING PA. (U) AEROSPACE CORP EL SEGUNDO
CA CHEMISTRY AND PHYSICS LAB D E COOPER ET AL.

1/1

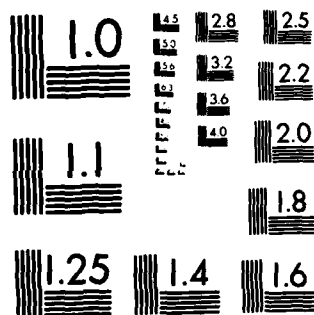
UNCLASSIFIED

30 JUN 86 TR-0086(6945-06)-1 SD-TR-86-36

F/G 9/1

NL

END
DATE
FILMED
10-86



XEROCOPY RESOLUTION TEST CHART
NATIONAL BUREAU OF STANDARDS-1963-A

AD-A170 618

**Picosecond Optoelectronic Measurement
of the High Frequency Scattering
Parameters of a GaAs FET**

**D. E. COOPER and S. C. MOSS
Chemistry and Physics Laboratory
Laboratory Operations
The Aerospace Corporation
El Segundo, CA 90245**

15 June 1986

**Prepared for
SPACE DIVISION
AIR FORCE SYSTEMS COMMAND
Los Angeles Air Force Station
P.O. Box 92960, Worldway Postal Center
Los Angeles, CA 90009-2960**

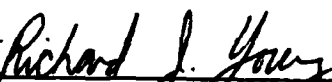
**APPROVED FOR PUBLIC RELEASE;
DISTRIBUTION UNLIMITED**

This report was submitted by The Aerospace Corporation, El Segundo, CA 90245, under Contract No. F04701-85-C-0086 with the Space Division, P.O. Box 92960, Worldway Postal Center, Los Angeles, CA 90009-2960. It was reviewed and approved for The Aerospace Corporation by S. Feuerstein, Director, Chemistry and Physics Laboratory.


Lt Richard J. Young/CGXT was the project officer for the Mission-Oriented Investigation and Experimentation (MOIE) Program.

This report has been reviewed by the Public Affairs Office (PAS) and is releasable to the National Technical Information Service (NTIS). At NTIS, it will be available to the general public, including foreign nationals.

This technical report has been reviewed and is approved for publication. Publication of this report does not constitute Air Force approval of the report's findings or conclusions. It is published only for the exchange and stimulation of ideas.



RICHARD J. YOUNG, Lt, USAF
MOIE Project Officer
SD/CGXT



JOSEPH HESS, GM-15
Director, AFSTC West Coast Office
AFSTC/WCO OL-AB

UNCLASSIFIED

SECURITY CLASSIFICATION OF THIS PAGE (When Data Entered)

REPORT DOCUMENTATION PAGE		READ INSTRUCTIONS BEFORE COMPLETING FORM
1. REPORT NUMBER SD-TR-86-34	2. GOVT ACCESSION NO. AD-A170618	3. RECIPIENT'S CATALOG NUMBER
4. TITLE (and Subtitle) PICOSECOND OPTOELECTRONIC MEASUREMENT OF THE HIGH FREQUENCY SCATTERING PARAMETERS OF A GaAs FET		5. TYPE OF REPORT & PERIOD COVERED
7. AUTHOR(s) Donald E. Cooper and Steven C. Moss		6. PERFORMING ORG. REPORT NUMBER TR-0086(6945-06)-1
9. PERFORMING ORGANIZATION NAME AND ADDRESS The Aerospace Corporation El Segundo, Calif. 90245		8. CONTRACT OR GRANT NUMBER(s) F04701-85-C-0086
11. CONTROLLING OFFICE NAME AND ADDRESS Space Division Los Angeles Air Force Station Los Angeles, Calif. 90009-2960		10. PROGRAM ELEMENT, PROJECT, TASK AREA & WORK UNIT NUMBERS
14. MONITORING AGENCY NAME & ADDRESS (if different from Controlling Office)		12. REPORT DATE 15 June 1986
		13. NUMBER OF PAGES 24
		15. SECURITY CLASS. (of this report) Unclassified
		15a. DECLASSIFICATION/DOWNGRADING SCHEDULE
16. DISTRIBUTION STATEMENT (of this Report) Approved for Public Release; Distribution Unlimited		
17. DISTRIBUTION STATEMENT (of the abstract entered in Block 20, if different from Report)		
18. SUPPLEMENTARY NOTES		
19. KEY WORDS (Continue on reverse side if necessary and identify by block number) Picosecond Optoelectronic Microwave Diagnostics Scattering Parameters		
20. ABSTRACT (Continue on reverse side if necessary and identify by block number) In this report, we present picosecond optoelectronic measurements of the pulse response of an unpackaged GaAs field effect transistor (FET). The data are transformed to the frequency domain to extract scattering parameters with >60 GHz bandwidth. Because of the large bandwidth available and simple de-embedding procedures, this is a very promising technique for characterization of devices operating in the millimeter-wave region.		

DD FORM 1473
(FACSIMILE)

UNCLASSIFIED

SECURITY CLASSIFICATION OF THIS PAGE (When Data Entered)

CONTENTS

I.	INTRODUCTION.....	5
II.	EXPERIMENTAL.....	7
III.	RESULTS AND DISCUSSION.....	13
IV.	CONCLUSIONS.....	23
	REFERENCES.....	25

Applicable For	
None	<input checked="" type="checkbox"/>
Partial	<input type="checkbox"/>
Unlimited	<input type="checkbox"/>
Justification	
For	
Introduction/	
Special Codes	
and/or	
List	
A-1	



FIGURES

1.	Experimental Arrangement Used to Measure the Response of Ultrafast Electronic Device.....	8
2.	Experimental Test Fixtures: (a) Split Fixture, (b) Planar Fixture.....	10
3.	GaAs FET (Avantek AT-8041, 0.5 μm Long Schottky Barrier Gate) Epoxied into Planar Test Fixture and Wire Bonded to Microstrips.....	12
4.	Transient Response of GaAs FET in Split Text Fixture: (a) Pulse and Sample Gate; (b) Pulse Drain, Sample Gate; (c) Pulse Gate, Sample Drain; (d) Pulse and Sample Drain.....	14
5.	Transient Response of GaAs FET in Planar Test Fixture: (a) Pulse and Sample Gate; (b) Pulse Drain, Sample Gate; (c) Pulse Gate, Sample Drain; (d) Pulse and Sample Drain.....	15
6.	S-Parameters for GaAs FET in Planar Test Fixture: (a) S_{11} ; (b) S_{12} ; (c) S_{21} ; (d) S_{22}	19

I. INTRODUCTION

Picosecond optoelectronics provides the capability to significantly advance the characterization of high frequency solid state devices. Time domain waveform measurements with a resolution of a few picoseconds can be transformed into scattering parameters with a bandwidth much greater than that obtained with conventional methods. The de-embedding of a device response from that of the circuit of the test fixture is also simplified by this technique. These advances have resulted from the application of mode-locked lasers¹ to the generation and measurement of short electrical pulses.²⁻⁹ In this report we apply these techniques to characterize solid state devices in terms that are useful to an electrical engineer.

Purely electronic time domain techniques have been used for device characterization for nearly two decades.¹⁰ Electronic pulse or step generators are used in conjunction with sampling oscilloscopes to achieve diagnostic accuracy and bandwidth comparable to conventional frequency domain analyzers. The bandwidth is limited by the response times of these components, with step recovery diodes producing electrical pulses 65 psec wide, and tunnel diodes generating step waveforms with 20 psec rise times.¹⁰ Sampling oscilloscopes have 20-30 psec rise times. Experimental and data analysis techniques have been developed to use these components to measure scattering parameters.¹¹ Despite these efforts, frequency domain measurement has been the most common approach to device characterization. The principal advantage of the time domain technique was the low cost of the pulse generators compared to the high cost of the continuous wave (cw) frequency generators needed for frequency domain diagnostics. Present frequency domain technology is limited to a 26 GHz bandwidth. Higher frequencies can be covered with frequency mixing techniques at the cost of additional noise and experimental complexity. However, advances in pulse generation and sampling now make the time domain techniques superior in bandwidth to the frequency domain approach. Thus, the preferred diagnostic technique for high frequency devices may become time

domain measurements. Recently, purely electronic techniques have advanced to ~ 2 psec resolution with the development of Josephson junctions,¹² although cryogenic temperatures are necessary for these devices.

Picosecond optoelectronic techniques for the generation and sampling of electrical pulses with a resolution of less than 10 psec were developed by Auston at Bell Laboratories.²⁻⁴ The picosecond optoelectronic measurement of the impulse response of a field effect transistor (FET) was one of the first applications of these methods.¹³ The excellent temporal resolution of this technique derives from the use of ultrashort optical pulses from mode-locked lasers interacting with photoconductive and electro-optic materials. Radiation damaged InP photoconductors have been used to generate pulses several volts in amplitude and about 1 psec in duration.⁵ Electro-optic sampling techniques based upon the Pockels effect have demonstrated temporal resolution of about $1/2$ psec. These advances, combined with the data analysis techniques developed to support the purely electronic time domain methods, can extend the diagnostic bandwidth to well beyond 100 GHz. In addition to the superior bandwidth of picosecond optoelectronic diagnostics, the de-embedding of the device from the test fixture is simplified because the pulse generator and sampler can be a few millimeters from the device being tested. Thus it is unnecessary to pass high frequency signals through connectors and long transmission lines. Because of these advantages, time domain analysis with picosecond optoelectronics is a very promising technique for characterizing advanced high frequency solid state devices.¹⁴⁻¹⁶ The picosecond optoelectronic technique is especially useful for characterization of nonlinear devices, where time domain analysis is the preferred approach.

In this report, we present picosecond optoelectronic measurements of the scattering parameters of a FET at frequencies up to and beyond 60 GHz. We discuss the advantages of this technique for de-embedding, and we indicate improvements that could be made to better adapt the test fixture to typical FET designs.

II. EXPERIMENTAL

Picosecond electrical pulses are produced and sampled by the illumination of ultrafast photoconductive switches with picosecond optical pulses. The illumination of a photoconductive material in the gap between two microstrips changes the conductivity of the gap region. When one of the microstrips has a direct current (dc) bias voltage applied to it, the transient photoconductivity of the gap launches an electrical pulse along the other microstrip. The temporal width of this pulse is determined by the temporal width of the optical pulse that illuminates the gap as well as by the response time of the photoconductive material in the gap. Electrical pulses with widths as short as a few picoseconds have been generated in this manner. A pulse generated at a first switch can then be sampled at a second switch. The second switch is illuminated by a second optical pulse that can be temporally delayed with respect to the first optical pulse. The second switch samples the voltage resulting from the ultrafast electrical pulse during the temporal aperture produced by the transient photoconductivity of the gap. Consequently, standard picosecond optical pump and probe techniques can generate and sample picosecond electrical pulses. For example, such techniques have been used to measure the dispersion of picosecond electrical pulses after propagation along various lengths of microstrip.¹⁷⁻¹⁹ Furthermore, the transient response of ultrafast electronic devices can be determined by placing the device between two of the switches just described and by measuring the reflected and transmitted electrical pulses. This technique has previously been used to measure the transient response of a packaged GaAs FET.¹³ In this report, we present the measurement of the ultrafast transient response of an unpackaged GaAs FET placed in two test fixtures incorporating the switches just described. We characterize the device response as well as the effects of each fixture on the device response.

As shown in Fig. 1, a train of picosecond optical pulses is produced by a dye laser (Rhodamine 6G or Styryl 9) pumped synchronously by an actively mode locked argon ion laser. The average output power was maximized in each case

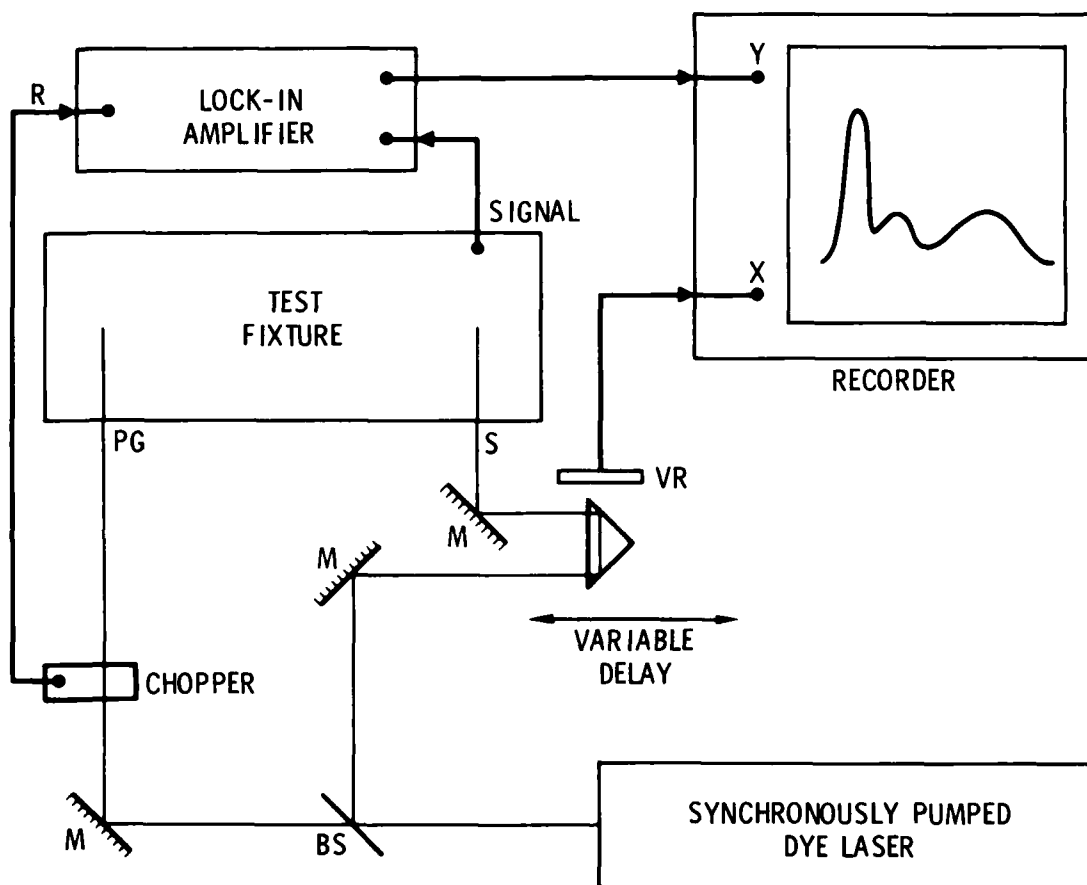


Fig. 1. Experimental Arrangement Used to Measure the Response of Ultrafast Electronic Devices. M-mirrors, BS-beamsplitter, PG-electrical pulse generator, S-electrical pulse sampler, VR-voltage ramp, R-reference from chopper.

by adjusting a three plate, intracavity birefringent tuning element. The temporal pulse width of the dye laser pulses was measured to be ~ 4 psec using a crossed beam second harmonic autocorrelation technique. The period between pulses in the train was ~ 4.3 nsec. The pulse train was split into two parts. Each part was directed separately onto one of the test fixtures. One beam, used to generate picosecond electrical pulses, propagated along a fixed path through a mechanical chopper and was focused onto a photoconductive switch on the test fixture. This beam line was mechanically chopped at 808 Hz with a 50% duty cycle. The second beam, used to produce the sampling aperture, traveled along a path of variable length determined by the position of a mechanical translation stage and was focused onto a second photoconductive switch on the test fixture. The peak fluence at each switch was $\sim 15 \mu\text{J}/\text{cm}^2$. The translation stage permits 8.3 cm travel. Consequently, the electrical signal at the sampling switch can be measured before, during, and for several hundred picoseconds after generation. This signal was monitored with a lock-in amplifier referenced to the chopper frequency. The output of the lock-in amplifier was fed into the y-axis input of an x-y recorder. The x-axis input was obtained from a voltage ramp controlled by the position of the translation stage. This arrangement provided a sensitive measurement of the output of the test fixture as a function of time delay between generating and sampling pulses.

We applied this technique to determine the impulse response of an unpackaged GaAs FET (Avantek AT-8041, $0.5 \mu\text{m}$ long Schottky barrier gate) that was embedded in one of two different test fixtures, as shown in Fig. 2. Photoconductive pulse generators and samplers were fabricated in microstrip transmission lines on silicon-on-sapphire (SOS) substrates. The gold microstrips were 1500 \AA thick. Bonding of the gold to the silicon was facilitated with a 50 \AA layer of chromium between the gold microstrip and the silicon. The test fixtures were ion implanted ($10^{15} \text{ O}^+ \text{ cm}^{-2}$ at 400 keV) to permit the generation of 6 to 7 psec electrical pulses. The temporal width of the electrical pulses did not depend strongly on whether the switches were illuminated with 560 nm light or with 820 nm light. Each test fixture had two central microstrips to control the operating point of the FET and four side

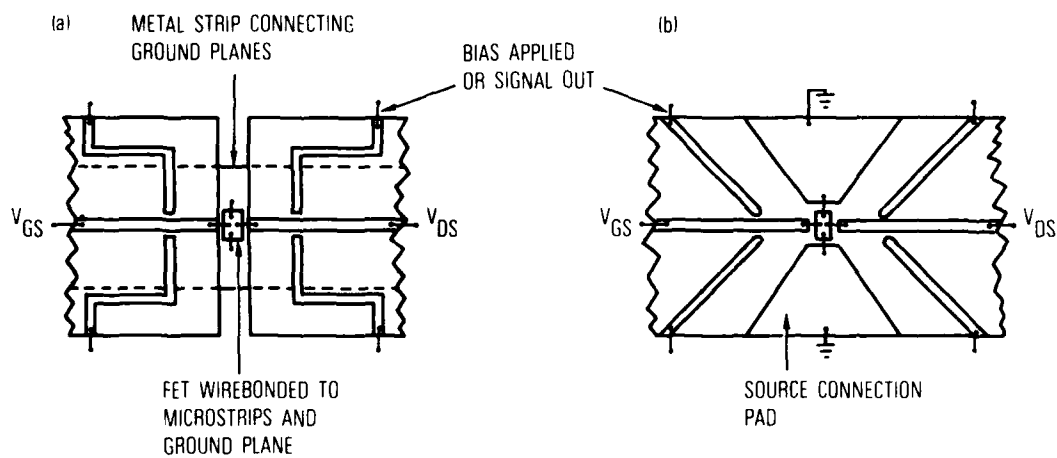


Fig. 2. Experimental Test Fixtures: (a) Split Fixture, (b) Planar Fixture

microstrips to permit the various reflection and transmission coefficients (i.e., scattering parameters) to be monitored for this two-port device. The electrical pulses were generated by illuminating the 25 μm gap between the central microstrips and one of the side microstrips, which was biased at +40 V. The microstrip impedance in each test fixture was $\sim 50\ \Omega$.

In the split fixture (Fig. 2a), two separate SOS wafers were connected by a gold plated Kovar strip attached to each ground plane with conducting epoxy. The substrates were 180 μm thick, and the photoconducting layer of silicon was 1 μm thick. The FET was epoxied to the $\sim 1\ \text{mm}$ gap between wafers. The gate and drain pads of the FET were wire bonded to the central microstrips on each side, and the source pads were wire bonded to the ground plane. The microstrips were 180 μm wide to preserve 50 Ω impedance.

The planar fixture design (Fig. 2b) was used to simplify fixture fabrication and reduce the inductance of the source bond wires. This design was fabricated on a single SOS wafer. The substrate was 250 μm thick, and the photoconducting layer of silicon was 1 μm thick. The FET was epoxied into the gap between the two central microstrips. Again the gate and drain pads were wire bonded to the central microstrips. However, in this fixture, the source connections were to the two large relatively low impedance trapezoidal shaped gold pads. Furthermore, the ends of the side microstrips were slightly rounded on this fixture to reduce the large edge effects observed in the split fixture. The microstrips were 250 μm wide to preserve 50 Ω impedance. The GaAs FET bonded into the test fixture is shown in Fig. 3.

In each fixture, the operating point of the FET was controlled by dc voltages applied to the gate and drain microstrips. The absolute magnitude of the input and output electrical signals was determined by referencing the measured signal levels to those obtained with a $\pm 10\ \text{mV}$ square wave signal on the central microstrip.



Fig. 3. GaAs FET (Avantek AT-8041, 0.5 μ m Long Schottky Barrier Gate) Epoxied into Planar Test Fixture and Wire Bonded to Microstrips

III. RESULTS AND DISCUSSION

The pulse response of an Avantek AT-8041 in the split test fixture is shown in Fig. 4, and the comparable data with the planar fixture are shown in Fig. 5. All these measurements were performed with the drain-to-source voltage at 3.0 V, and the drain current was 30 mA. Results depicted in the a and d portions of both figures were produced by reflecting an electrical pulse off the gate or drain, respectively. For these measurements the pulses are generated at one port of the device, and sampling is done at the same port immediately opposite the pulse generation switch. Thus the large initial peak represents the profile of the pulse as it is generated, corresponding to an optoelectronic autocorrelation measurement.⁴ The shoulder on the trailing edge of the pulse profile is caused by a reflection at the wire bond to the microstrip. The broad signal at later times is the result of the reflection from the FET and contains the information about the device response. Finally, the split fixture exhibits an oscillatory signal that is attributed to a reflection in the microstrip circuit. A comparison of these signals from the two test fixtures reveals two major differences. First, the shoulder on the autocorrelation peak is better resolved in the planar test fixture because there is a longer section of microstrip between the optoelectronic switches and the wire bond. Second, the oscillatory artifact has been eliminated in the planar fixture by straightening the side microstrips that carry the switch bias voltage. Because of these improvements, the data from the planar test fixture are much easier to analyze.

In Figs. 4 and 5, signal b indicates the result of injecting a pulse into the drain port and sampling the gate response. These signals have almost no dc component when transformed to the frequency domain, because the gate is capacitively coupled to the rest of the transistor. The shape of these signals varies with the bias voltages and currents, which indicates that they are affected by variations in device capacitances and transconductance.¹¹ The differences in the waveforms for the two fixtures are attributed to the different test circuits, in particular the different source connections.

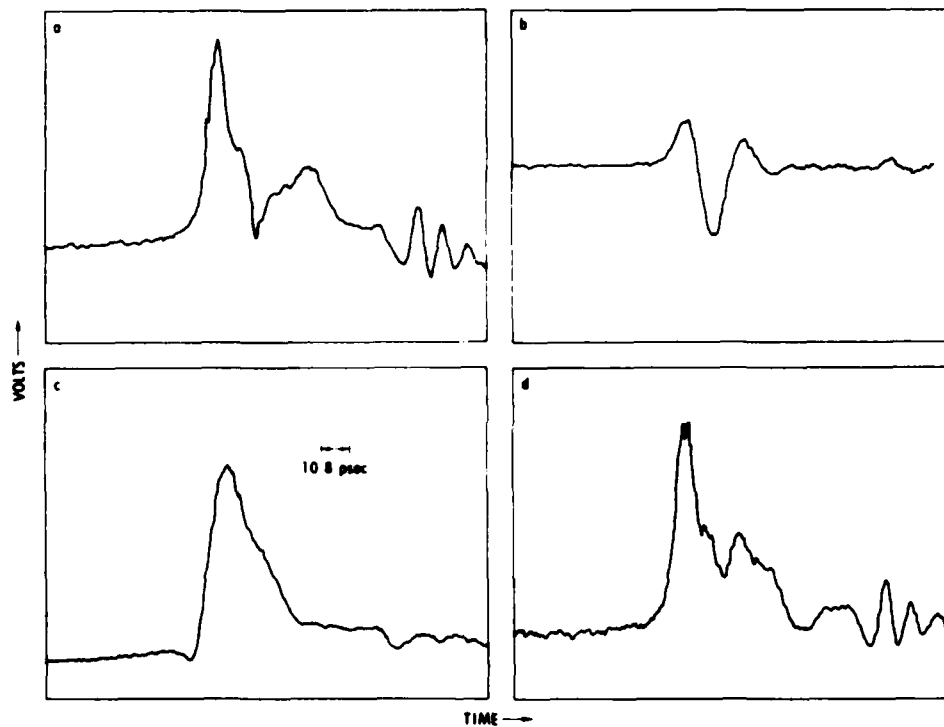


Fig. 4. Transient Response of GaAs FET in Split Test Fixture: (a) Pulse and Sample Gate; (b) Pulse Drain, Sample Gate; (c) Pulse Gate, Sample Drain; (d) Pulse and Sample Drain

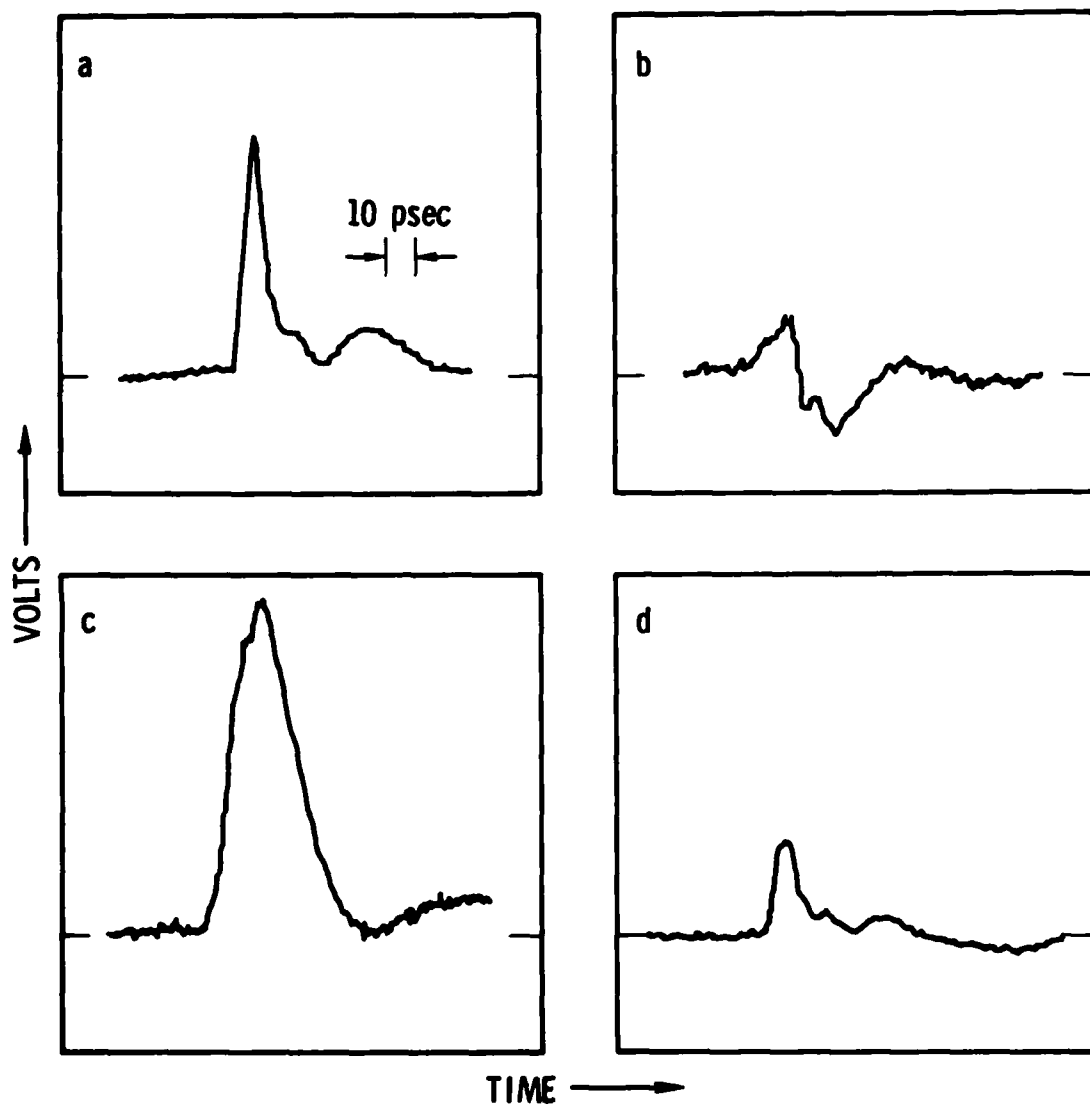


Fig. 5. Transient Response of GaAs FET in Planar Test Fixture: (a) Pulse and Sample Gate; (b) Pulse Drain, Sample Gate; (c) Pulse Gate, Sample Drain; (d) Pulse and Sample Drain

In Figs. 4 and 5, waveform c exhibits the result of amplifying a pulse by injecting it into the gate and sampling the drain response. The split fixture (Fig. 4c) produced an 8.2 psec rise time, which is close to the limit of temporal resolution for our equipment and is the fastest temporally resolved FET rise time of which we are aware. The source bond wires for this measurement were unusually long (~ 1 mm), which may have lowered the gain and contributed a high frequency resonance to produce the very rapid rise time. In the planar test fixture, the source bond wires were much shorter (~ 350 μ m). The resultant waveform has a 15 psec rise time. The input and output sampling switches were calibrated for this measurement, and the peak output pulse voltage was 1.5 times that of the input pulse.

Finally, we note the presence of a strong background signal in the electrical reflectivity measurements that was not present in the electrical transmission measurements. This background may have been caused by light passing through the silicon epilayer in the gap at the pulse generating switch, reflecting off the ground plane and illuminating the sampling switch. In the reflectivity measurements, the pulse generator and pulse sampler are separated by only the width of the central microstrip, whereas in the transmission measurements they are considerably further apart. The constant background level was subtracted before data analysis.

Analysis of the time domain data to recover the frequency domain scattering parameters followed the methods developed for purely electronic time domain measurements. A magnetostrictive digitizer connected to a microcomputer was used to digitize the data at 256 points along the waveform. Each point was separated from the next by 1.055 psec. A fast Fourier transform (FFT) was performed to extract the frequency domain information. Consequently, the discrete frequency spectrum obtained consisted of 129 points, each separated from the next by ~ 3.7 GHz, beginning at 0.0 GHz. The temporal spacing is small enough to prevent aliasing.¹⁰ In each case discussed in this report, the spectrum drops to noise levels well before the end of its range. Finally, the data were normalized to correct for the finite temporal widths of the input pulse and the sampling aperture. The spectra of the reflected signals were normalized by simply dividing by the corresponding

spectrum of the waveform of the input pulse. The spectra of the transmitted signals were normalized by dividing by the harmonic mean of the spectra obtained from input pulses on both sides of the device. The harmonic mean was then normalized to the amplitude of the appropriate input. Whereas this procedure accounts for the possibility that switches separated by a considerable distance may have different temporal responses, it does not account for the possibility that generating and sampling switches on the same side of the device may have different responses. However, this possibility may be tested by generating and sampling pulses at each switch, in turn, and comparing the results. The result of this data analysis is the frequency spectrum of one of the four scattering parameters. S_{11} is derived from the reflection of a pulse off the gate (Figs. 4a and 5a), and S_{22} is measured by reflecting a pulse off the drain (Figs. 4d and 5d). S_{21} and S_{12} are measured by passing a pulse through from the gate to the drain or vice versa, respectively (Figs. 4c and 4b, and Figs. 5c and 5b). Thus the device can be completely characterized by these four pulse response measurements.

The normalized FFT of the device pulse response is a complex function of the frequency and thus contains both amplitude and phase information. The magnitude of the normalized FFT is the gain or the reflection coefficient. The phase angle is also an important parameter to measure. A discussion of the determination of the phase factors illustrates the ease with which de-embedding can be done with the picosecond optoelectronic technique. In a Fourier transformation, a temporal delay transforms into a phase shift with frequency. Thus quantitative measurement of the phase factors requires determination of the temporal origin of the time domain waveforms. If we refer to Fig. 4a or Fig. 5a, the temporal origin is clearly marked by the optoelectronic autocorrelation peak. Using this peak as the temporal origin fixes the reference plane at the optoelectronic switches. Subtracting this peak from the waveform yields the pulse response for a system consisting of a short length of microstrip, a bond wire, and the FET connected to the rest of the circuit. Ideally one would like to measure only the pulse response of the FET. The de-embedding process consists of measurements and data manipulation intended to mathematically eliminate the effects of the other components. In

our measurements, we approximate the microstrip as a dispersionless transmission line that adds only a propagation delay to the time domain data. The propagation constant of the microstrip is measured in a separate experiment,¹⁷ and the temporal origin of the waveform is shifted to compensate for the appropriate length of microstrip. Thus the effects of the microstrip are mathematically removed, and the reference plane is moved up to the microstrip-wire bond interface. The same temporal origin (corresponding to a position of the optical delay line) was used for the calculation of all four scattering parameters.

Additional data manipulation can be performed through time domain windowing. This process removes waveform regions that are identified with electrical components other than the device being tested. An example is the subtraction of the autocorrelation peak from the reflection waveforms. This technique could be applied to the microstrip-wire bond reflection, because it is unrelated to the FET itself. However, the pulses reflected from the FET must pass through this interface. Thus, windowing of this reflection would not remove all the effects of the interface. Furthermore, we wished to reproduce as nearly as possible the measurements performed by the manufacturer, which included this interface. A better technique for de-embedding the wire bond would be to characterize a wire bond of the same length that connects the microstrip to the ground plane. In any case, the picosecond optoelectronic technique results in very simple de-embedding procedures and is particularly suited to time domain windowing.

Figure 6 exhibits the scattering parameters calculated from the pulse response of the FET in the planar test fixture. The manufacturer's scattering parameters (measured by conventional means) are also shown, although the two sets of data are not directly comparable because of the different test fixtures used. In particular, the source connection in our planar test fixture was made to a pad with a width-to-substrate thickness ratio of 3, which yields a 25Ω impedance when considered as a transmission line. There are probably also variations in bond wire lengths that could have a considerable effect on the reflection measurements. In spite of these problems, the agreement between the two sets of scattering parameters is fairly good for the transmission measurements.

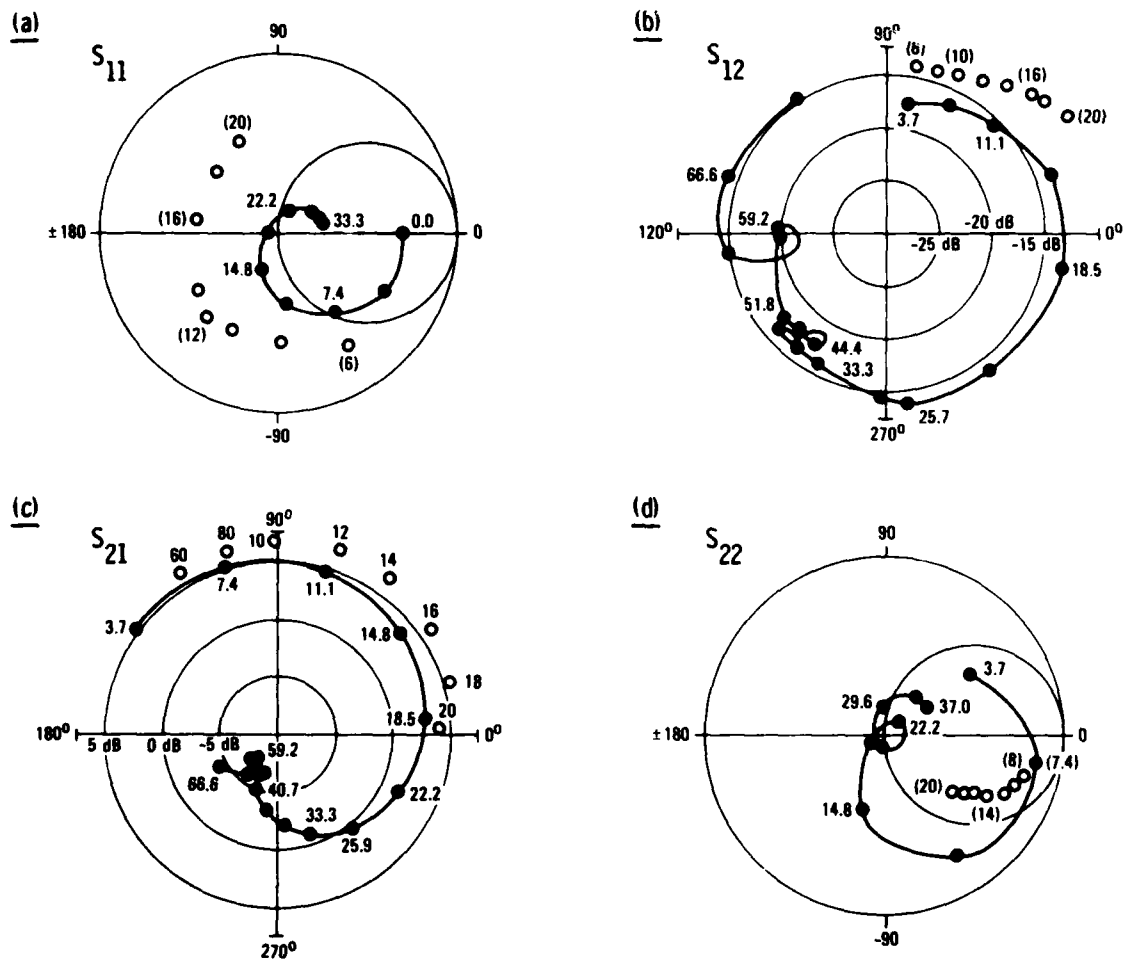


Fig. 6. S-Parameters for GaAs FET in Planar Test Fixture: (a) S_{11} ; (b) S_{12} ; (c) S_{21} ; (d) S_{22} . Closed circles - our data, open circles - manufacturer's data.

Figure 6c is a polar plot of S_{21} , in which the picosecond optoelectronic data are compared with the manufacturer's measurements. The fit over the 6-20 GHz region is quite good, with somewhat less gain indicated in our measurements. This may be a result of the large source impedance in our test fixture. The phase factors agree very well, indicating that the two methods of measuring the propagation delay yield the same result. Beyond the bandwidth limit of the manufacturer's specifications, the picosecond optoelectronic data cross through the 0 dB gain line at about 27 GHz, which is typical for a GaAs FET with a 0.5 μm gate. The complicated double resonance at 50 to 60 GHz is attributed to the quarter wave resonances of the gate and drain bond wires. The data continue to be well above the noise level out beyond 60 GHz.

Figure 6b is a polar plot of S_{12} calculated from the data of Fig. 5b. The fit to the manufacturer's measurements is fairly good at low frequencies, although there is considerably more phase shift at frequencies approaching 20 GHz. At higher frequencies the same resonances seen in the S_{12} data appear near 40 and 60 GHz.

Figures 6a and 6d exhibit the Smith charts for S_{11} and S_{22} , respectively. In both plots, the data beyond about 35 GHz fall within a very small region on the chart, so the data were truncated there to avoid congestion. The poor fit between the picosecond optoelectronic data and the manufacturer's specifications is probably the result of differences in the way the FET was bonded to the surrounding circuit. The main features of our results can be understood in terms of the time domain data (Figures 5a and 5d), which in both cases consist of a reflection at the wire bond-microstrip interface followed about 25 psec later by a broad peak representing the reflection from the device itself. This transforms into low amplitude frequency components at around 20 GHz, where points on a wave separated by 25 psec are of opposite polarity. The scattering parameter amplitudes rise again beyond this point and converge on a small region of the chart. This is because all the high frequency components arise from the relatively sharp reflection from the interface rather than the broad device reflection. The reference plane is at this interface, so that the temporal origin is at this sharp reflection peak. Thus there is no propagation delay, which means no phase shift as a

function of frequency. This results in the congested group of high frequency points near the real axis. The Smith charts of S_{11} and S_{22} accurately reflect the main features of the interface between the device and the microstrip circuit of the test fixture.

IV. CONCLUSIONS

We have illustrated the application of picosecond optoelectronics to high frequency device diagnostics by characterizing a $0.5\text{ }\mu\text{m}$ GaAs FET. Pulse response measurements were transformed into scattering parameters, which completely define the device performance in the linear regime. A bandwidth of greater than 60 GHz results from the application of pulse generation and sampling techniques based upon the use of ultrashort laser pulses. De-embedding is also simplified because the pulses are generated and sampled a few millimeters from the device being tested. Because of these advantages, picosecond optoelectronics is a very promising technique for device diagnostics in the millimeter wave region.

The test fixture is a very important component for device diagnostics, because it determines the circuit that surrounds the device. The split test fixture used in our studies is quite suitable for some devices, such as vertical FETs²⁰ or permeable base transistors.²¹ In these devices, the ground contact is on the bottom, conveniently situated for the split fixture. In the standard planar FETs, the source pads are on the top at either side, and low impedance connection to the ground plane represents a problem in designing integrated circuits as well as test fixtures. One possible solution is the use of a coplanar waveguide transmission line structure,²² in which the ground plane is located on either side of the central conductor. We are investigating the use of coplanar waveguide for picosecond optoelectronic device diagnostics.

In addition to the capabilities we have illustrated in measuring the linear properties of devices, picosecond optoelectronics can be very useful in studying nonlinear devices such as power FETs. In nonlinear systems, frequency domain analysis is not valid, and direct time domain analysis is necessary. The current theoretical models of nonlinear effects in solid state devices are quite cumbersome, and contributions from time domain experiments on nonlinear devices may result in a better understanding of nonlinear effects.

In summary, we have presented picosecond optoelectronic pulse response measurements on a 0.5 μm gate GaAs FET and have transformed the results into scattering parameters. The useful bandwidth is over 60 GHz, more than twice that of conventional cw diagnostic techniques. We discussed the importance of the experimental test fixture and the advantages of the picosecond optoelectronic technique in de-embedding the device from the test fixture. Picosecond optoelectronics will be very useful in the characterization of millimeter-wave devices, especially nonlinear devices where conventional frequency-domain techniques are not applicable.

REFERENCES

1. D. H. Auston and K. B. Eisenthal, eds., Ultrafast Phenomena IV, Springer-Verlag, New York (1984), pp. 2-104.
2. D. H. Auston, "Picosecond Optoelectronic Switching and Gating in Silicon," Appl. Phys. Lett. 26, 101-103 (1975).
3. P. R. Smith, D. H. Auston, A. M. Johnson, and W. M. Augustyniak, "Picosecond Photoconductivity in Radiation-Damaged Silicon-on-Sapphire Films," Appl. Phys. Lett. 38, 47-50 (1981).
4. D. H. Auston, "Impulse Response of Photoconductors in Transmission Lines," IEEE J. Quantum Electron. QE-19, 639-648 (1983).
5. P. M. Downey and B. Tell, "Picosecond Photoconductivity Studies of Light-Ion-Bombarded InP," J. Appl. Phys. 56, 2672-2674 (1984).
6. R. B. Hammond, N. G. Paulter, R. S. Wagner, and W. R. Eisenstadt, "Integrated Picosecond Photoconductors Produced on Bulk Si Substrates," Appl. Phys. Lett. 45, 404-405 (1984).
7. J. A. Valdmanis, G. A. Mourou, and C. W. Gabel, "Subpicosecond Electrical Sampling," IEEE J. Quantum Electron. QE-19, 664-667 (1983).
8. F. J. Leonberger and P. F. Moulton, "High-Speed InP Optoelectronic Switch," Appl. Phys. Lett. 35, 712-714 (1979).
9. C. H. Lee and V. K. Mathur, "Picosecond Photoconductivity and Its Applications," IEEE J. Quantum Electron. QE-17, 2098-2112 (1981).
10. J. R. Andrews, "Automatic Network Measurements in the Time Domain," Proc. IEEE 66, 414-423 (1978); and references therein.
11. S. Y. Liao, Microwave Devices and Circuits, Prentice-Hall, Englewood Cliffs, New Jersey (1980).
12. P. Wolf, "Picosecond Sampling with Josephson Junctions," in Picosecond Electronics and Optoelectronics, Springer-Verlag, New York (1985), pp. 236-243.
13. J. K. A. Everard and J. E. Carroll, "Practical Comparison of Optoelectronic Sampling Systems and Devices," Proc. IEEE 130, pt. I, 5-16 (1983).
14. K. E. Meyer, D. R. Dykaar, and G. A. Mourou, "Characterization of TEGFETs and MESFETs Using the Electro-Optic Sampling Technique," in Picosecond Electronics and Optoelectronics, Springer-Verlag, New York (1985), pp. 54-57.

15. D. E. Cooper and S. C. Moss, "Picosecond Optoelectronic Diagnostics of Field Effect Transistors," in Picosecond Electronics and Optoelectronics, Springer-Verlag, New York (1985), pp. 62-65.
16. D. E. Cooper, "Picosecond Optoelectronic Measurement of Microstrip Dispersion," Appl. Phys. Lett. 47 (in press).
17. G. Hasnain, G. Arjavalingam, A. Dienes, and J. R. Whinnery, "Dispersion of Picosecond Pulses on Microstrip Transmission Lines," Proc. SPIE 439, 159-163 (1983).
18. J. A. Valdmanis, G. Mourou, and C. W. Gabel, "Subpicosecond Electrical Sampling," Proc. SPIE 439, 142-148 (1983).
19. P. R. Smith, D. H. Auston, and W. M. Augustyniak, "Measurement of GaAs Field-Effect Transistor Electronic Impulse Response by Picosecond Optical Electronics," Appl. Phys. Lett. 39, 739-741 (1981).
20. T. M. S. Heng and H. C. Nathanson, "Vertical MOS Transistor Geometry for Power Amplification at Gigahertz Frequencies," Electronics Lett. 10, 490-492 (1974).
21. C. O. Bozler and G. D. Alley, "The Permeable Base Transistor and Its Application to Logic Circuits," Proc. IEEE 70, 46-52 (1982).
22. C. P. Wen, "Coplanar Waveguide: a Surface Strip Transmission Line Suitable for Nonreciprocal Gyromagnetic Device Applications," IEEE Trans. Microwave Theory Tech. MTT-17, 1087-1090 (1969).

LABORATORY OPERATIONS

The Aerospace Corporation functions as an "architect-engineer" for national security projects, specializing in advanced military space systems. Providing research support, the corporation's Laboratory Operations conducts experimental and theoretical investigations that focus on the application of scientific and technical advances to such systems. Vital to the success of these investigations is the technical staff's wide-ranging expertise and its ability to stay current with new developments. This expertise is enhanced by a research program aimed at dealing with the many problems associated with rapidly evolving space systems. Contributing their capabilities to the research effort are these individual laboratories:

Aerophysics Laboratory: Launch vehicle and reentry fluid mechanics, heat transfer and flight dynamics; chemical and electric propulsion, propellant chemistry, chemical dynamics, environmental chemistry, trace detection; spacecraft structural mechanics, contamination, thermal and structural control; high temperature thermomechanics, gas kinetics and radiation; cw and pulsed chemical and excimer laser development including chemical kinetics, spectroscopy, optical resonators, beam control, atmospheric propagation, laser effects and countermeasures.

Chemistry and Physics Laboratory: Atmospheric chemical reactions, atmospheric optics, light scattering, state-specific chemical reactions and radiative signatures of missile plumes, sensor out-of-field-of-view rejection, applied laser spectroscopy, laser chemistry, laser optoelectronics, solar cell physics, battery electrochemistry, space vacuum and radiation effects on materials, lubrication and surface phenomena, thermionic emission, photo-sensitive materials and detectors, atomic frequency standards, and environmental chemistry.

Computer Science Laboratory: Program verification, program translation, performance-sensitive system design, distributed architectures for spaceborne computers, fault-tolerant computer systems, artificial intelligence, microelectronics applications, communication protocols, and computer security.

Electronics Research Laboratory: Microelectronics, solid-state device physics, compound semiconductors, radiation hardening; electro-optics, quantum electronics, solid-state lasers, optical propagation and communications; microwave semiconductor devices, microwave/millimeter wave measurements, diagnostics and radiometry, microwave/millimeter wave thermionic devices; atomic time and frequency standards; antennas, rf systems, electromagnetic propagation phenomena, space communication systems.

Materials Sciences Laboratory: Development of new materials: metals, alloys, ceramics, polymers and their composites, and new forms of carbon; non-destructive evaluation, component failure analysis and reliability; fracture mechanics and stress corrosion; analysis and evaluation of materials at cryogenic and elevated temperatures as well as in space and enemy-induced environments.

Space Sciences Laboratory: Magnetospheric, auroral and cosmic ray physics, wave-particle interactions, magnetospheric plasma waves; atmospheric and ionospheric physics, density and composition of the upper atmosphere, remote sensing using atmospheric radiation; solar physics, infrared astronomy, infrared signature analysis; effects of solar activity, magnetic storms and nuclear explosions on the earth's atmosphere, ionosphere and magnetosphere; effects of electromagnetic and particulate radiations on space systems; space instrumentation.

DATE
FILMED
0-8